Distinctive diffusion regimes of organic molecules in clays: (de)coupled motion with water

Eduardo Duque-Redondo[†,*], Iñigo López-Arbeloa[†] and Hegoi Manzano[‡]

†Molecular Spectroscopy Laboratory, Department of Physical Chemistry, University of the Basque Country UPV/EHU, Aptdo. 664, 48080, Bilbao, Spain.

‡Department of Condensed Matter Physics, University of the Basque Country UPV/EHU, Aptdo. 664, Bilbao, Spain.

The combination of organic and inorganic components enables the development of new generation of materials with innovative applications in many fields. Clays are commonly used to confine different ions and molecules since they act as an engineering barrier, avoiding the release of the entrapped species. In this work, we have employed molecular dynamics simulations to study the diffusivity of a variety of organic molecules enclosed in the interlaminar space of clays. We have found that the diffusivity of the organic molecules follows a universal trend, exhibiting low diffusion coefficients at low water contents, which are radically increased at a certain water content. This onset of diffusion is due to the rearrangement of the water molecules from monolayer to bilayer. At that point, the motion of the water/guest molecule cluster is decoupled, leading to the sharp increase of the diffusion coefficients.

Introduction

The design of new materials based on organic-inorganic complexes has demonstrated an outstanding potential for novel and improved applications in many areas of material science, medicine, energy, optics, electronics or environmental protection[1–5]. Among the inorganic substrates, clays show great versatility due to their swelling properties and high cation adsorption capacity, which provide the possibility of confining a large number of species in their interlaminar spaces. Nevertheless, to ensure a good performance of the organic-clay systems it is necessary to maintain a constant concentration of the organic compounds during its operative life, avoiding leaking processes that can affect to the global workability. Moreover, clays have low hydraulic permeability in a saturated state, acting as a barrier avoiding the migration of the confined species and providing a very efficient isolation[6,7]. However, the diffusive processes that takes place in the interlaminar spaces of clays may affect to the final properties of the hybrid materials. Although the diffusion of alkali and alkaline earth cations in clays has been studied in depth[8–10], little work has been done in the study processes that governs the diffusivity of organic molecules encapsulated in clays at molecular scale.

In this paper, we have employed molecular dynamics to study the dynamics of organic guest molecules confined in the interlaminar space of clays. For that purpose, we built hybrid systems based on two common smectite clays, Laponite and saponite, that accommodate in their interlaminar space different organic molecules and a variable water content, from 1.25 to 10 M_{water}/M_{clay}. We have chosen a variety of guest molecules with structural dissimilarities, as well as different sizes and charges. These differences allow to draw a global diffusive behaviour for organic molecules embedded in clays, providing new insights into the diffusion mechanisms of adsorbed organic molecules.

Atomistic model and simulation details

As starting point, we employed the structures of hectorite (natural analogous of synthetic Laponite) and saponite described by Breu[12] and Rayner[13], respectively. We modified the chemistry to obtain a stoichiometry in Laponite of $[Na_{0.83}][Mg_{5.17}Li_{0.83}][Si_8]O_{20}(OH)_4$ and $[Na_{0.83}][Mg_6][Si_{7.17}Al_{0.83}]O_{20}(OH)_4$ for saponite. The simulation cell consisted of 24 unit cells, with a size about 2.1 x 1.8 nm^2 in the basal plane and 3.4 nm in the perpendicular direction. The clay layers exhibit a net negative charge as a consequence of the isomorphic substitutions of Mg^{2+} by Li^+ and Si^{4+} by Al^{3+} in Laponite and saponite, respectively. The excess of negative charge is compensated with Na^+ exchangeable cations to maintain the electroneutrality of the system. The organic molecules were built using Avogadro and relaxed using density functional theory (DFT) B3LYP/6-311+G(d,p) simulations as implemented in Gaussian[14]. The charges were computed using the electro-static potential (ESP) fitting method[15].

Among the organic molecules under study (see **Figure 1a**), there are cationic dyes, such as pyronin-Y and LDS-722, both with excellent fluorescent properties[2]; commonly-used surfactants of different length and charge, as N,N-dimethyloctadecylamine, N,N-dimethyldodecylamine and N,N,N-trimethyloctadecylammonium; and as benzo(a)pyrene, a carcinogen aromatic polycyclic molecule[11]. On the other hand, the two smectite clays selected (see **Figure 1b**) differ in the charge distribution in their sheets. Laponite presents an aliovalent substitution in the octahedral sheet, replacing Mg^{2+} partially by Li^+ atoms, originating a negative charge excess in this

inner sheet. In contrast, saponite has a partial substitution of Si^{4+} by Al^{3+} in the tetrahedral layer, leading to a negative charge in the external layers. In this way, these two clays enable the evaluation of the effect of the charge distribution in the diffusion properties. Besides that, increasing water content allows to ascertain the role of the water in the dynamics of the guest molecules.

The relaxed organic molecules were inserted into the interlaminar spaces of Laponite and saponite. For each organic molecule we performed 8 simulations with different water contents from 1.25 to

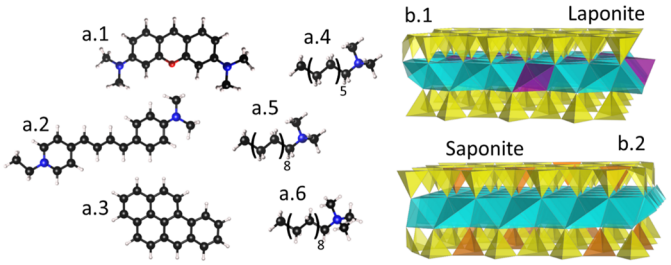

Figure 1. Representation of the guest molecules: (a.1) pyronin-Y, (a.2) LDS-722, (a.3) benzo(a)pyrene, (a.4) N,N-dimethyldodecylamine, (a.5) N,N-dimethyloctadecylamine and (a.6) N,N,N-trimethyloctadecylammonium; and the clays: (b.1) Laponite and (b.2) saponite. In the organic molecules, the black, blue, red and white balls represent C, N, O and H atoms. In the clay structures, the yellow and orange tetrahedrons correspond to silicate and aluminate chains, whereas the blue and purple octahedrons represent the Mg and Li layers.

10 M_{water}/M_{clay} increasing in regular amounts of 1.25 M_{water}/M_{clay}. A total of 96 simulations were carried out, measuring the interlaminar spaces and computing the diffusion coefficients of the guest molecules for each of them. LAMMPS simulation package[16] was used to carry out the molecular dynamics (MD) simulations. ClayFF[17], CHARMM[18] and SPC[19] force fields were used to describe the bonding interactions in clays, organic and water molecules, respectively. The combination of those force fields has been previously used and proved appropriate to model hybrid systems with clays, water and organic molecules[20–24].

All the simulated systems were initially minimized, relaxing both the box parameters and the atomic positions. Afterwards, molecular dynamics in the canonical ensemble (NVT) was performed at 300K during 250 ps. It was used a thermostat coupling constant of 0.1 ps and a time step of 1 fs, using Verlet algorithm[25] for the integration of the equations of motion. Then, the atomic positions and volume were equilibrated under room conditions (300K and 1 atm) turning to the isobaric-isothermal ensemble (NPT) during 1 ns. Finally, a canonical ensemble was carried out during 0.1 μs for obtaining reliable computed diffusion constants.

Results and discussion

Basal distances. After the equilibration of the systems, we have analysed first the variation of the basal distances as the water content is increased. **Figure 2** shows that the expansion produced by water is uniform for all the systems, independently of the organic molecule incorporated. The expansion of the interlaminar space of both clays is about 4.5Å from the lowest water content, 1.25 M_{water}/M_{clay}, to the highest one, 10 M_{water}/M_{clay}. However, the widening of the interlaminar space is not linear with the water addition. There is an abrupt expansion in both clays from 5 to 6.5 M_{water}/M_{clay}. This anomaly has been attributed to the process of rearrangement of the water molecules located in the interlaminar space of the clays as the water content increases[26,27]. In order to verify that the sharp increase in the basal distance is caused by a water rearrangement, we have computed the density profiles of interlayer spaces.

Density profiles. The density profiles enable the study of the water

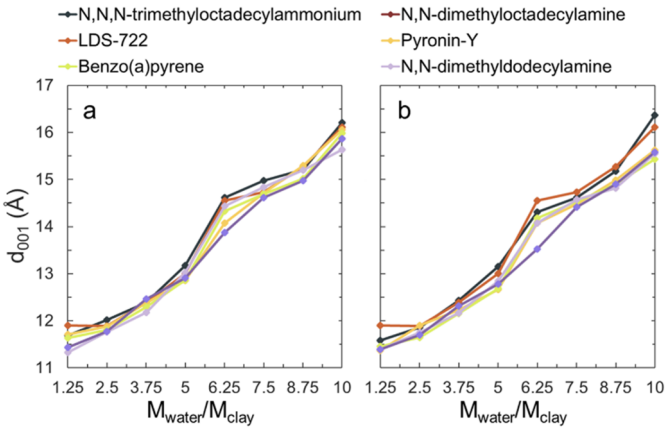

Figure 2. Basal distance evolution as the water content increases for the different studied systems in (a) Laponite and (b) saponite.

structure in the interlaminar space and its evolution as the water content grows. Likewise, this tool is very useful to evaluate the distribution of the guest organic molecules in the clay slit pores and how they are affected by the water content. The distribution of the water and organic molecules in the interlaminar space for Laponite and saponite at different water contents is shown in **Figure 3**.

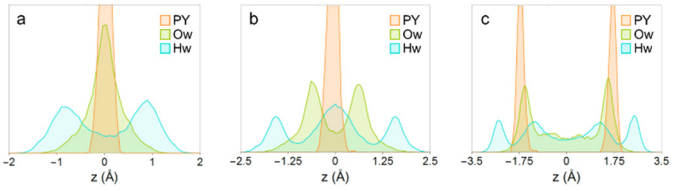

Figure 3. Density profiles of the interlaminar space of Laponite that incorporates pyronin-Y as function of z distance for (a) 1, (b) 1.5 and (c) 2 water layers. In orange are shown the profile of pyronin-Y molecules, the water oxygen and hydrogen atoms are in green and blue. The zero corresponds to the centre of the interlaminar space.

At low water contents, a perfect water monolayer is observed up to 3.1 M_{water}/M_{clay}. Above this limit, the water monolayer evolves to a bilayer, with intermediate distributions, reaching a perfect water bilayer at water contents about 5.6 M_{water}/M_{clay}. It is remarkable that the incorporation of the organic molecules do not modify substantially the water arrangement reported for unmodified clays[28,29]. The monolayer and bilayer distribution are stable hydration states and consequently water molecules tend to maintain those distributions[29]. In a monolayer distribution, water molecules are able to establish hydrogen bonds with the two clay surfaces that define the interlaminar space, while they can only form hydrogen bonds with only one surface in a bilayer distribution. Thus, as the water content increases, these molecules tend to maintain the monolayer distribution, although distorted, until it is more favourable the organization in a bilayer. This transition from monolayer to bilayer causes the abrupt rise in the basal distance.

The water arrangement determines the distribution of the guest molecules in the interlaminar space. At low water concentration, the organic molecules are aligned in the middle of the pore with the water molecules. However, when the pore is expanded due to water incorporation, the organic compounds tends to stay close to the clay sheets due to its hydrophobicity as can be seen in **Figure 3**. This behavior is analogous in both clays for all the studied molecules.

Diffusion coefficients. We have computed the mean square displacement (MSD) in order to obtain the diffusion coefficients of the species confined in the clays. The plot of the evolution of the diffusion coefficients as the water content increases, **Figure 4**, clearly shows that the water arrangement has a significant impact. The diffusivity of the organic molecules in the water monolayer regime is very low, but their diffusion coefficients are gradually increased as the water content grows. When the water bilayer regime is reached, there is a sharp increase of the diffusion coefficients, up to two orders of magnitude higher than in the monolayer regime. It is worth highlighting that the guest molecules confined in our systems exhibit a universal behaviour in their diffusivity, independently of their size, charge or structure flexibility, and it is also found in both clays, Laponite and saponite.

The diffusion coefficients of all the organic molecules are in the same range, with small variations due to their different size and structure. In Laponite, it is possible to establish an inverse relationship between diffusion coefficients and molecular weight and/or volume: the higher the size of the organic molecule, the lower its diffusivity. In saponite, this relationship is not as clear as in Laponite. This may be due to the different distribution of the negative charge in the sheets of those clays. In saponite, the negative charge is located in the tetrahedral layers, the external ones, where in Laponite the charge is in the internal layer, in the octahedral layers. In order to evaluate the effect of the charge distribution in the clay sheets we have compared the evolution of the diffusion coefficients of the guest molecules in Laponite and saponite. It can be seen in **Figure 4 (c)** that the location of the charge in the clays has no noticeable impact on the diffusivity of N,N-dimethyloctadecylamine, a neutral molecule. In contrast, this effect is remarkable in case of LDS-722, a charged molecule, as it is shown in **Figure 4 (d)**. Neutral molecules do not establish intense electrostatic interactions with the charged surfaces of saponite. However, the electrostatic interactions between charged molecules and surfaces are particularly intense and consequently, reduce the mobility of charged species[23]. Thus, the strong interactions between the charged LDS-722 and the charged surface of saponite cause a decrease of diffusion coefficients in comparison with Laponite.

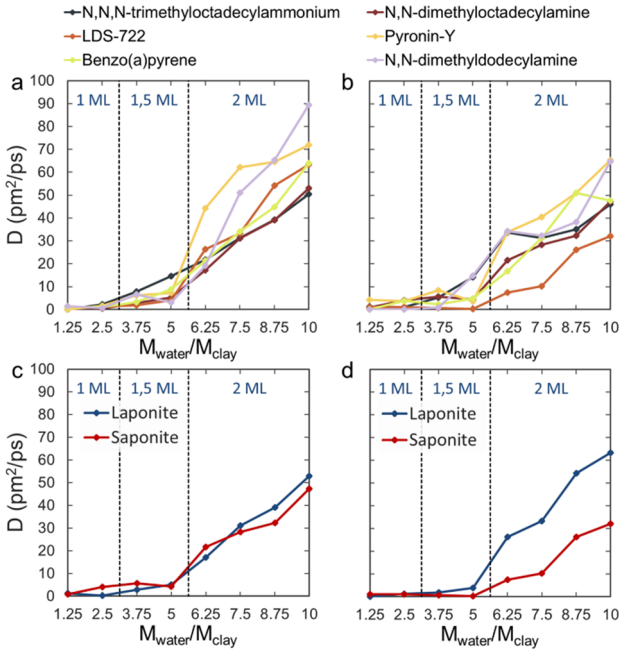

Figure 4. Evolution of the diffusion coefficients of the organic molecules under study at different M_{water}/M_{clay} in **(a)** Laponite and **(b)** saponite. Comparison of the diffusion coefficients for **(c)** a neutral molecule, N,N-dimethyloctadecylamine and **(d)** a charged one, LDS-722 in Laponite (blue lines) and saponite (red lines).

It might be thought that the abrupt expansion of the interlaminar space in the transition from water monolayer to bilayer may favour the motion of the guest molecules not only in the parallel plane to the clay sheets, but also in the perpendicular direction to them, hindered at low water contents. However, the analysis of the diffusivity decomposed in the x, y and z axis shows that the motion of the guest molecules is scarcely increased in the perpendicular direction to the clay sheets. For instance, the diffusion in z direction of benzo(a)pyrene (**Figure 5 (a)**) does not change significantly as the interlaminar space is expanded, while the diffusion parallel to the clay sheets increases gradually. This results in diffusivities three orders of magnitude lower in the perpendicular direction to the clay sheets than in the parallel ones. Nevertheless, at high water contents, it has been observed zigzagging motion in the z axis of the guest molecules, whereas at low water contents, the motion in that direction is limited, as can be seen in **Figure 5 (b)**. The jumps from the proximities of one clay layer to the other are due to hydrophobic character of the guest molecules. However, these jumps barely contribute to the diffusivity because, despite the expansion of the interlaminar space since the distances that the molecules travels in

the z-direction are much smaller than the distances covered in the xy plane.

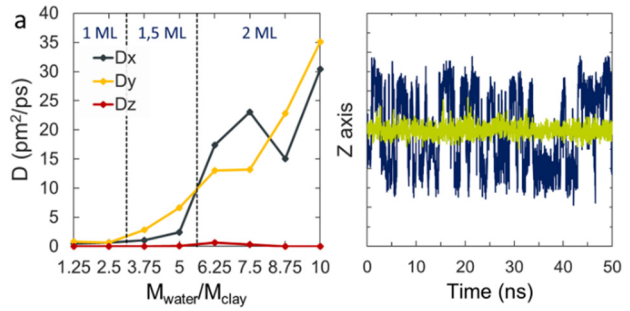

Figure 5. (a) Benzo(a)pyrene motion with respect to the z axis, perpendicular to the clay sheets. Green and red colours are referred to low and high water contents, respectively. **(b)** Decomposed diffusion coefficients in x, y and z axis for benzo(a)pyrene molecules in Laponite.

(De)coupled water-guest molecule motion. At low water content water must flow around the guest molecules in the same plane, while at high water content, water can flow also below or above of the guest molecules. We hypothesized that such a degree of freedom could be the origin of the diffusion increase. We have computed the combined distribution function of displacement and lifetime for water-organic molecules clusters in order to evaluate if water and guest molecules move coupled or not. **Figure 6 (a)** shows that at low water contents, water and organic molecules behave as a cluster, exhibiting a coupled motion up to 3.5 ns. These clusters cover small distances of about 1 nm as a consequence of the low diffusion coefficients. On the other hand, at higher water contents (**Figure 6 (b)**), the organic and water molecules remain together less than 0.5 ns, seven times less than at low water contents, but they cover together higher distances. Therefore, the high lifetimes indicate that the motion of water and organic molecules is coupled at low water contents, but as the water content is increased, the motion of the guest molecules is decoupled from the motion of water, enabling greater freedom of those molecules. This results in the increase of the diffusion coefficients of both water and organic molecules.

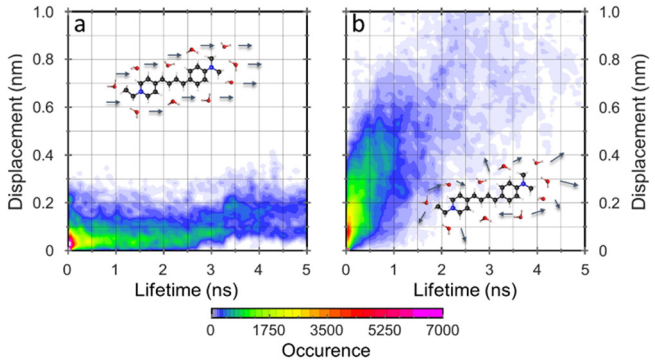

Figure 6. Combined distribution functions of displacement and lifetime for water-organic molecules clusters at (a) low and (b) high water content for the LDS molecules adsorbed in Laponite.

Conclusions

In this work, we have employed molecular dynamics to study at atomic level the processes that govern the diffusivity of the organic molecules encapsulated in clay slit pores. For that purpose, we built systems based on Laponite and saponite clays with a variety of organic molecules, ranging from dyes, surfactants to aromatic polycyclic compounds. The different structure, flexibility, charge and size of the organic compounds under study allows to define a common diffusive behavior for guest molecules occluded in clays as a function of the water content.

It is remarkable that we have found a universal diffusive trend for the confined organic molecules. At low water contents, the diffusion coefficients of these species are very low, but increase progressively as water is added. As with the basal distances, the diffusion coefficients increase drastically when the bilayer regime is reached. The analysis of the diffusion in each direction has shown that only the diffusion in the parallel plane to the clay contributes significantly to the global diffusivity. The analysis of the lifetimes and distances covered by water-organic compounds clusters indicates that their motion is coupled only at low water content, in the monolayer regime, but is decoupled at higher water contents, in bilayer regime. The evolution from a jammed stated when the interlayer molecules' motion is coupled to a loose state when it is decoupled might be the ultimate reason of the increase of the diffusion coefficients.

The results of this work shed light on the diffusion of organic molecules confined in clays. The universal trend found in the diffusive behavior of these molecules could be possibly extrapolated to organic molecules encapsulated in other hydrophilic laminar systems.

Author information

*E-mail: eduardo.duque@ehu.eus

Acknowledgements

This work was supported by "Departamento de Educación, Política Lingüística y Cultura del Gobierno Vasco" (IT912-16) and the ELKARTEK program. E.D.-R. acknowledge the "Contrato de Personal Investigador Predoctoral en Formación" from the UPV/EHU, respectively. The authors thank for technical and human support provided by IZO-SGI SGIker of UPV/EHU and European funding (ERDF and ESF), as well as the i2basque computing resources.

References

1 T. Polubesova, S. Nir, D. Zadaka, O. Rabinovitz, C. Serban, L. Groisman and B. Rubin, *Environ. Sci. Technol.*, 2005, **39**, 2343–2348.

2 N. Epelde-Elezcano, V. Martinez-Martinez, E. Duque-Redondo, I. Temiño, H. Manzano and I. López-Arbeloa, *Phys.*

Chem. Chem. Phys., 2016, **18**, 8730–8738.
3 S.-H. Cheng, C.-H. Lee, C.-S. Yang, F.-G. Tseng, C.-Y. Mou and L.-W. Lo, *J. Mater. Chem.*, 2009, **19**, 1252–1257.
4 J.-M. Zen and C.-W. Lo, *Anal. Chem.*, 1996, **68**, 2635–2640.
5 J. Gong, J. Liang and K. Sumathy, *Renew. Sustain. Energy Rev.*, 2012, **16**, 5848–5860.
6 A. Meunier, B. Velde and L. Griffault, *Clay Miner.*, 1998, **33**, 187–196.
7 F. T. Madsen, *Clay Miner.*, 1998, **33**, 109–129.
8 G. Kosakowski, S. V Churakov and T. Thoenen, *Clays Clay Miner.*, 2008, **56**, 190–206.
9 P. Leroy, A. Revil and D. Coelho, *J. Colloid Interface Sci.*, 2006, **296**, 248–255.
10 V. Marry and P. Turq, *J. Phys. Chem. B*, 2003, **107**, 1832–1839.
11 Q. Ba, J. Li, C. Huang, H. Qiu, J. Li, R. Chu, W. Zhang, D. Xie, Y. Wu and H. Wang, *Environ. Health Perspect.*, 2015, **123**, 246.
12 J. Breu, W. Seidl and A. Stoll, *Z. anorg. allg. Chem.*, 2003, **629**, 503–515.
13 J. H. Rayner, *Min. Mag.*, 1974, **39**, 850–856.
14 M. Frisch, G. W. Trucks, H. B. Schlegel, G. E. Scuseria, M. A. Robb, J. R. Cheeseman, G. Scalmani, V. Barone, B. Mennucci and G. A. Petersson, *Inc., Wallingford, CT*, 2009, **200**.
15 U. C. Singh and P. A. Kollman, *J. Comput. Chem.*, 1984, **5**, 129–145.
16 S. Plimpton, *J. Comput. Phys.*, 1995, **117**, 1–19.
17 R. T. Cygan, J.-J. Liang and A. G. Kalinichev, *J. Phys. Chem. B*, 2004, **108**, 1255–1266.
18 A. D. MacKerell, D. Bashford, M. Bellott, R. L. Dunbrack, J. D. Evanseck, M. J. Field, S. Fischer, J. Gao, H. Guo and S. a Ha, *J. Phys. Chem. B*, 1998, **102**, 3586–3616.
19 H. J. C. Berendsen, J. P. M. Postma, W. F. van Gunsteren and J. Hermans, in *Intermolecular forces*, Springer, 1981, pp. 331–342.
20 S. Kang, T. Huynh, Z. Xia, Y. Zhang, H. Fang, G. Wei and R. Zhou, *J. Am. Chem. Soc.*, 2013, **135**, 3150–3157.
21 J. A. Greathouse and R. T. Cygan, *Phys. Chem. Chem. Phys.*, 2005, **7**, 3580–3586.
22 R. Zhu, W. Chen, T. V Shapley, M. Molinari, F. Ge and S. C. Parker, *Environ. Sci. Technol.*, 2011, **45**, 6504–6510.
23 X. Liu, L. Wang, Z. Zheng, M. Kang, C. Li and C. Liu, *J. Hazard. Mater.*, 2013, **244**, 21–28.
24 E. Duque-Redondo, H. Manzano, N. Epelde-Elezcano, V. Martínez-Martínez and I. López-Arbeloa, *Chem. Mater.*, 2014, **26**, 4338–4345.
25 H. Grubmüller, H. Heller, A. Windemuth and K. Schulten, *Mol. Simul.*, 1991, **6**, 121–142.
26 D. E. Smith, *Langmuir*, 1998, **14**, 5959–5967.
27 K. Kawamura, Y. Ichikawa, M. Nakano, K. Kitayama and H. Kawamura, *Eng. Geol.*, 1999, **54**, 75–79.
28 L. J. Michot, A. Delville, B. Humbert, M. Plazanet and P. Levitz, *J. Phys. Chem. C*, 2007, **111**, 9818–9831.
29 J. Breu, W. Seidl, A. J. Stoll, K. G. Lange and T. U. Probst, *Chem. Mater.*, 2001, **13**, 4213–4220.